Dalton Transactions

PAPER

View Article Online
View Journal | View Issue



Cite this: *Dalton Trans.*, 2017, **46**, 1618

# *In situ* ligand exchange-mediated 0D/1D transformation of a polyoxovanadate†

M. Wendt,[a] P. Polzin,[a] J. van Leusen,[b] C. Näther,[a] P. Kögerler*[b] and W. Bensch*[a]

Received 21st November 2016,
Accepted 10th January 2017

DOI: 10.1039/c6dt04412c

rsc.li/dalton

The antimonato-polyoxovanadate $\{Ni^{II}(en)_3\}_3[V^{IV}_{15}Sb^{III}_6O_{42}(H_2O)]\cdot ca.15H_2O$ was utilized as a synthon for the solvothermal *in situ* generation of the new compound $\{Ni^{II}(phen)_3\}_2[\{Ni^{II}(en)_2\}V^{IV}_{15}Sb^{III}_6O_{42}(H_2O)]\cdot 19H_2O$, a rearrangement induced by ligand metathesis. While in the precursor structure cations and anions are isolated, the solid-state structure of the product is characterized by 1D chains consisting of alternating $[V_{15}Sb_6O_{42}(H_2O)]^{6-}$ cluster shells and $[Ni(en)_2]^{2+}$ units covalently linked to neighboring clusters *via* terminal oxygen atoms. Water clusters composed of sixteen hydrogen-bonded $H_2O$ molecules are located in void spaces of the structure. The magnetic properties indicate weak antiferromagnetic interactions of the bridging $Ni^{2+}$ center and adjacent polyoxovanadate anions, as well as small magnetic anisotropy of the individual $Ni^{2+}$ centers.

## Introduction

The structures and physico-chemical properties of high-nuclearity polyoxovanadate (POV) clusters can be significantly altered by introducing hetero-atoms like *e.g.* Si, Ge, As, or Sb.[1] Charge compensation of the negatively charged POV clusters is realized by ammonium,[2–4] alkali metals cations,[5–8] protonated amine molecules[9–12] or transition metal amine complexes.[13–15] There are also reports that bond formation between the POV cores and cations[16–18] leads to charge-neutral complexes. The main synthetic route for preparation of such hetero-POVs is the solvothermal approach applying vanadium and antimony compounds such as $NH_4VO_3$, $V_2O_5$ or $Sb_2O_3$ as educts. Hetero-POVs are synthesized at pH > 8 using $V^V$-containing sources, and a reducing agent is required for generation of the magnetically highly interesting partially reduced or fully reduced compounds, *i.e.* those comprising $V^{IV}$ centers. Hence, the POV chemistry significantly differs from polyoxomolybdate and polyoxotungstate chemistry, where preformed cluster anions or *in situ* generated building blocks are used as synthons for the preparation of chemically modified high-nuclearity clusters.

Recently, we discovered a Sb-POV exhibiting good solubility in water.[19] In a first synthesis we reacted this compound, $\{Ni(en)_3\}_3[V_{15}Sb_6O_{42}(H_2O)]\cdot ca.15H_2O$ (**I**), at $T$ = 150 °C leading to *in situ* reorganization of the cluster shell and formation of the β-isomer of the $[V_{14}Sb_8O_{42}]^{4-}$ anion.[20] In the presence of $[Ni(phen)_3](ClO_4)_2\cdot 0.5H_2O$ (phen = 1,10-phenanthroline) and $Sb_2O_3$ the α-isomer of $[V_{14}Sb_8O_{42}]^{4-}$ could be obtained.[21]

To further develop this Sb-POV chemistry, we reacted **I** with $[Ni(phen)_3](ClO_4)_2\cdot 0.5H_2O$, which leads to the formation of the new compound $\{Ni(phen)_3\}_2[\{Ni(en)_2\}V_{15}Sb_6O_{42}(H_2O)]\cdot 19H_2O$ (**II**). The partial replacement of the $[Ni(en)_3]^{2+}$ complexes in **I** here leads to interconnection of the $\{V_{15}Sb_6O_{42}\}$ anions into a 1D chain-based solid-state structure, in which large $(H_2O)_{16}$ water clusters are located. Here, we report the synthesis, crystal structure and the magnetic properties of the new compound $\{Ni(phen)_3\}_2[\{Ni(en)_2\}V_{15}Sb_6O_{42}(H_2O)]\cdot 19H_2O$ (**II**) representing the first successful *in situ* transformation of an isolated $\{V_{15}Sb_6O_{42}\}$ moiety into a higher hierarchical structure.

## Results and discussion

The title compound $\{Ni(phen)_3\}_2[\{Ni(en)_2\}V_{15}Sb_6O_{42}(H_2O)]\cdot 19H_2O$ (**II**) can be prepared according to several synthesis routes. Heating **I** for 1 d at 150 °C in the presence of pure phenanthroline, $[Ni(phen)_3]^{2+}$, $[Cr(phen)_2Cl_2]^{1+}$ or $[Eu(phen)_2(NO_3)_3]$ afforded formation of **II** (see Experimental section for details). The results of the different synthesis routes strongly indicate that an *in situ* ligand exchange reaction takes place.

Compound **II** crystallizes in the monoclinic space group $C2/c$ with four formula units per unit cell (Table S3†) with all atoms except V2, Ni1, O7, O13 and the oxygen water atoms O38–O42 located on general positions. The structure features the $[V_{15}Sb_6O_{42}(H_2O)]^{6-}$ cluster shell as central structural motif (Fig. 1). Two condensed $V_6$ hexagons formed by edge-sharing

[a]*Institute of Inorganic Chemistry, Christian-Albrechts University of Kiel, Max-Eyth-Str. 2, 24118 Kiel, Germany. E-mail: wbensch@ac.uni-kiel.de*
[b]*Institute of Inorganic Chemistry, RWTH Aachen University, Landoltweg 1, 52074 Aachen, Germany. E-mail: paul.koegerler@ac.rwth-aachen.de*

†Electronic supplementary information (ESI) available. CCDC 1504150. For ESI and crystallographic data in CIF or other electronic format see DOI: 10.1039/c6dt04412c

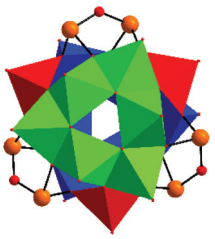

Fig. 1 Crystal structure of the cluster anion of $[V_{15}Sb_6O_{42}]^{6-}$ in **II**. The two $V_6$ hexagons and the three $VO_5$ pyramids joining the hexagons are drawn in different colors. Red: oxygen; orange: Sb (the central $H_2O$ molecule is omitted for clarity).

$VO_5$ polyhedra are joined by three $VO_5$ pyramids and three $Sb_2O_5$ units forming the sequence $V_6$–$V_3$–$V_6$ in the cluster anions. The terminal V=O bonds are shorter (average: 1.619 Å) than the bridging V–$\mu_3$-O bonds (average: 1.950 Å) (Table S4†). The Sb–O bonds scatter in a narrow range (1.930–1.944 Å; average: 1.938 Å, Table S4†). All geometric parameters of the anion agree well with literature data of Sb-POVs.[22–27] The oxidation states were determined by bond valance sum calculation (BVS)[28] leading to the formulation $[V^{IV}_{15}Sb^{III}_6O_{42}]^{6-}$ (Table S4†). The presence of $V^{IV}$ centers is supported by the strong characteristic vanadyl stretching vibration at 973 $cm^{-1}$ in the IR spectrum (Fig. S3†).

The cluster anions are joined by $[Ni(en)_2]^{2+}$ complex cations into chains that elongate along [101] with the $[Ni(phen)_3]^{2+}$ complexes 'decorating' the chains (Fig. 2 and S6†). The $Ni^{2+}$ cations are octahedrally coordinated by two en ligands and two O atoms from two adjacent *trans*-positioned polyanions. The Ni–N (2.085(3)–2.095(3) Å) and Ni–O bonds (2.158(2) Å) are in line with the literature.[29] In the crystallographically independent $[Ni(phen)_3]^{2+}$ complex, $Ni^{2+}$ is in a distorted octahedral environment with Ni–N bond lengths ranging from 2.079(3) to 2.114(3) Å, equatorial N–Ni–N angles between 79.01(12) and 98.58(13)°, and *trans* N–Ni–N angles from 166.96(13) to 171.66(13)° (see Table S5†).

Within the (101) plane a layered arrangement of alternating $[Ni(phen)_3]^{2+}$ complexes and chains is observed (Fig. 3).

The voids between the POV clusters (Fig. 3) are occupied by $(H_2O)_{16}$ clusters, consisting of two unique and seven symmetry-related $H_2O$ molecules (Fig. S7†). The geometric parameters of the hydrogen bonding interactions of the water cluster (Fig. 4) are listed in Table S7.† All values are typical for

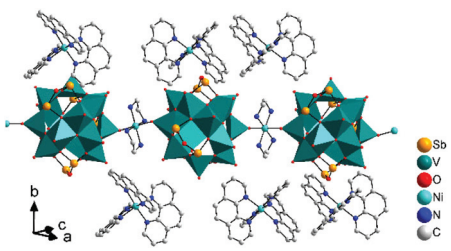


Fig. 2 Crystal structure of **II** with view of the chains and the decorating $[Ni(phen)_3]^{2+}$ complexes (H atoms are omitted for clarity).

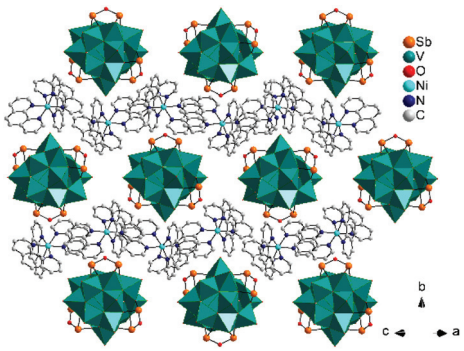


Fig. 3 View of the arrangement of the chains in the (101) plane (H atoms are omitted for clarity).

strong hydrogen bonds reported for water clusters.[30–34] Following the nomenclature suggested by Infantes *et al.*[35–37] the cluster can be defined as U0 type for cross-linked discrete rings, namely U02(2)2(2)5(2)5(2)5(3)5(3)8(6). The water cluster has a stabilizing effect caused by further H bonds to oxygen atoms of the Sb-POV cluster core, to O16 connecting the $\{V_{15}Sb_6O_{42}\}$ clusters with bridging $[Ni(en)_2]^{2+}$, and to the N–H atoms of the $[Ni(en)_2]^{2+}$ complex and to the C–H atoms of the $[Ni(phen)_3]^{2+}$ cations (Table S6†).

In many structures of POVs water molecules are observed, which are frequently disordered preventing the identification of water clusters. Hence, the occurrence of the $(H_2O)_{16}$ cluster is unusual in Sb-POV chemistry.

The remaining water molecules (O40 and O41) are not involved in H bonding interactions. Besides the hydrogen bonding network involving the water cluster, the $[Ni(en)_2]^{2+}$ and the $[Ni(phen)_3]^{2+}$ complexes form H bonds with oxygen atoms of the POV cluster shell (Table S7†). Furthermore, pronounced π–π stacking interactions between the aromatic phenanthroline ligands are present (Fig. 5). There are three types of intermolecular distances: sandwich type arrangements (average: 3.906 Å, shortest: 3.687 Å), parallel oriented phen molecules (average: 3.841 Å; shortest: 3.666 Å) and T-shaped arrangements (3.970 Å). For such π–π interactions, energies in the order of 10 kcal $mol^{-1}$ were calculated and significantly contribute to the structural arrangements.[38–42]

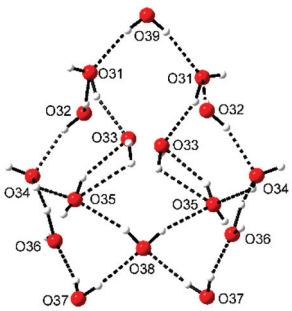


Fig. 4 Water cluster in **II** constructed by hydrogen bonding interactions between the water molecules located in the free spaces in Fig. 3 (red: O, gray: H).

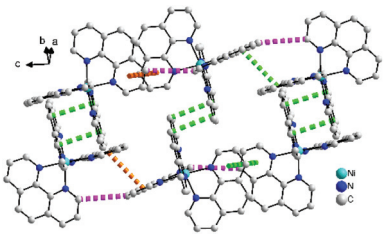


Fig. 5 Possible π–π stacking interactions between the aromatic phenanthroline ligands in the structure of **II** (T-shaped: pink, parallel: green, sandwich: orange).

During the transformation of $\{Ni(en)_3\}_3[V_{15}Sb_6O_{42}(H_2O)]\cdot ca.15H_2O$ (**I**) into $\{Ni(phen)_3\}_2[\{Ni(en)_2\}V_{15}Sb_6O_{42}(H_2O)]\cdot 19H_2O$ (**II**), two of the $[Ni(en)_3]^{2+}$ complexes are formally substituted by $[Ni(phen)_3]^{2+}$ complexes. The third $[Ni(en)_3]^{2+}$ complex loses one ethylenediamine ligand and connects adjacent anions to form a chain. The observation that not all en ligands in the $[Ni(en)_3]^{2+}$ complexes are exchanged is somewhat surprising because $[Ni(phen)_3]^{2+}$ was supplied in a threefold excess. The formation of an intermediate with composition $[\{Ni(en)_2\}V_{15}Sb_6O_{42}(H_2O)]^{4-}$ cannot be excluded. But based on our observations made in ref. 21 where **I** was transformed into the $[V_{14}Sb_8O_{42}]^{4-}$ cluster, the formation of such an intermediate is not likely. It seems that an en ligand of one of the $[Ni(en)_3]^{2+}$ complexes is detached followed by bond formation to POV oxygen sites. Applying $[Ni(phen)_3]^{2+}$ in the reaction the other $[Ni(en)_3]^{2+}$ complexes are either exchanged or en is replaced by phen. In addition, syntheses with phen, $[Cr(phen)_2Cl_2]^{1+}$ or $[Eu(phen)_2(NO_3)_3]$ also afforded crystallization of **II** requiring an *in situ* ligand exchange of en by phen.

Many Sb-POVs contain isolated cations and anions,[43–45] but 1D,[31,46] 2D [16] and 3D networks[17,27] are less common. Fig. 6 summarizes the structures obtained until now using **I** as synthon and $Ni^{2+}$-centered en and phen complexes. The compound $[\{Ni(en)_2\}_2V_{14}Sb_8O_{42}]\cdot 5.5H_2O$ [20] (**III**) crystallized with a Sb-richer cluster shell and the complexes join adjacent anions thus generating a layered structure. A different isomer of the $[V_{14}Sb_8O_{42}]^{4-}$ anion was observed in $\{Ni(phen)_3\}_2[V_{14}Sb_8O_{42}]\cdot phen\cdot 12H_2O$ [21] (**IV**), and cations and the anion are separated. In the title compound the cluster anion of the synthon is retained and the ligand exchange pattern yields a 1D structure.

To get a better understanding of the reaction conditions the ratio of precursor compound **I**: $[Ni(phen)_3](ClO_4)_2\cdot 0.5H_2O$ and the reaction temperature were altered. The lower the temperature, the lower was the yield, but **II** was always obtained between 80 and 140 °C. At the lowest temperatures compound **II** crystallized in a low yield in a mixture with the precursor **I**. Change of the ratio of the starting materials also leads to a lower yield, yet crystallization of **II** was always observed.

### Magnetic measurements

The temperature-dependent magnetic susceptibility data for compound **II** at 0.1 Tesla and the molar magnetization $M_m$ *vs.* magnetic field $B$ at 2.0 K are shown in Fig. 7. At 290 K, the $\chi_mT$ value of 6.11 $cm^3\ K\ mol^{-1}$ is higher than expected[47] for three non-interacting high-spin $Ni^{2+}$ centers (the expectation range for $Ni^{II}$ is 2.94–4.60 $cm^3\ K\ mol^{-1}$). Taking into account the contribution of 15 (hypothetically) non-interacting $V^{4+}$ centers, this value is, however, significantly below the corresponding expected range 8.36–10.22 $cm^3\ K\ mol^{-1}$. The deviation is readily explained by the magnetism of the $\{V_{15}Sb_6\}$ polyoxovanadate anion, as it is characterized as a system of 15 spin-1/2 vanadyl groups that exhibit strong antiferromagnetic coupling,[23] leading to low $\chi_mT$ values at room temperature. Upon decreasing the temperature, the $\chi_mT$ *vs.* $T$ curve for **II** is approximatively linear down to 25 K, and subsequently sharply decreases to 4.17 $cm^3\ K\ mol^{-1}$ at 2.0 K. The low-temperature

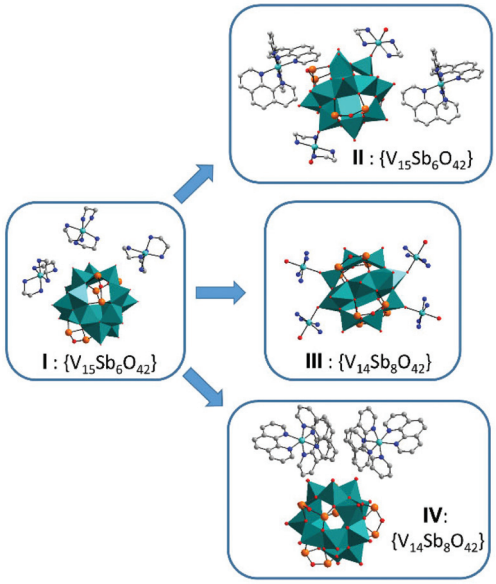


Fig. 6 Compounds derived from the precursor $\{Ni(en)_3\}_3[V_{15}Sb_6O_{42}(H_2O)]\cdot ca.15H_2O$ [19] (**I**): $\{Ni(phen)_3\}_2[\{Ni(en)_2\}V_{15}Sb_6O_{42}(H_2O)]\cdot 19H_2O$ (**II**), $[\{Ni(en)_2\}_2V_{14}Sb_8O_{42}]\cdot 5.5H_2O$ [20] (**III**) and $\{Ni(phen)_3\}_2[V_{14}Sb_8O_{42}]\cdot phen\cdot 12H_2O$ [21] (**IV**).

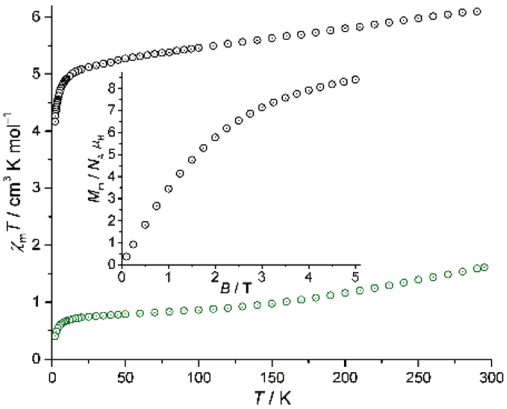


Fig. 7 Magnetic data of **II**: $\chi_mT$ *vs.* temperature $T$ at 0.1 T; inset: molar magnetization $M_m$ *vs.* magnetic field $B$ at 2.0 K. Black circles: experimental data; green circles: $\chi_mT([V_{15}Sb_6O_{42}]^{6-})$ (scaled).[23]

characteristics of $\chi_m T$ are potentially due to weak antiferromagnetic interactions of the bridging $Ni^{2+}$ center and the two neighboring polyoxovanadate anions as well as a small anisotropy of the single $Ni^{2+}$ centers due to ligand field effects and spin–orbit coupling. For $T > 25$ K, non-interacting octahedrally coordinated $Ni^{2+}$ centers are expected to yield an almost constant $\chi_m T$ *vs.* $T$ curve, thus the data seem to indicate a temperature-independent paramagnetic (TIP) contribution. This assumption is, however, disproved by the fact that the remaining $\chi_m T \approx 5.1$ cm$^3$ K mol$^{-1}$ is far too large for three $Ni^{2+}$ ions. In addition, we consider the magnetic data of the isolated $\{V_{15}Sb_6\}$ polyoxovanadate anion[23] depicted in Fig. 7 as green circles: on the one hand, the $\chi_m T$ *vs.* $T$ curve is not a straight line through the origin (which would correspond to a TIP). On the other hand, the distinct bend of the curve at approx. 160 K does not appear in the data for **II**. We thus assume that the bridging $Ni^{2+}$ center either affects the exchange interactions within the $\{V_{15}Sb_6\}$ anion, or this effect is directly due to the $\{V_{15}Sb_6\}$–Ni–$\{V_{15}Sb_6\}$ exchange pathway. The molar magnetization at 2.0 K (Fig. 7, inset) is a linear function of the applied field up to *ca.* 2 T, and reaches $M_m = 8.4 N_A \mu_B$ at 5.0 T without saturation. This value is larger than for the range 6.0–7.4 $N_A \mu_B$ expected for three non-interacting (or ferromagnetically coupled) $Ni^{2+}$ cations, therefore indicating a significant contribution caused by the $\{V_{15}Sb_6\}$ anions at 2.0 K. Using CONDON,[48,49] we explore several model scenarios to reproduce the magnetic data (see ESI†), but the simple model of additive contributions (of $Ni^{II}$ and $\{V_{15}Sb_6\}$), which usually works well for transition metal-augmented Sb-POVs, does not satisfactorily reproduce the magnetic characteristics of **II**.

## Conclusions

We demonstrated that the soluble precursor $\{Ni(en)_3\}_3[V_{15}Sb_6O_{42}(H_2O)]\cdot ca.15H_2O$ can be transformed *in situ* into $\{Ni(phen)_3\}_2[\{Ni(en)_2\}V_{15}Sb_6O_{42}(H_2O)]\cdot 19H_2O$ in the presence of phen or phen containing complexes within 1 d, a transformation that apparently is driven by step-wise ligand exchange. This reorganization of the constituents induces formation of a chain structure consisting of $Ni^{2+}$-centered complexes and anionic cluster shells, in which large and highly ordered water clusters are embedded. The usage of soluble precursors for the synthesis of new POV compounds leads to a dramatic shortening of the reaction time compared to usual POV synthesis.

## Experimental

Both precursor compounds $\{Ni(en)_3\}_3[V_{15}Sb_6O_{42}(H_2O)]\cdot ca.15H_2O$ (**I**) and $[Ni(phen)_3](ClO_4)_2\cdot 0.5H_2O$ were synthesized as described in literature.[19,50] The compound $\{Ni(phen)_3\}_2[\{Ni(en)_2\}V_{15}Sb_6O_{42}(H_2O)]\cdot 19H_2O$ (**II**) was prepared under solvothermal conditions in DURAN glass tubes (inner volume 11 mL) at 150 °C. $[Eu(phen)_2(NO_3)_3]$ was synthesized by dissolving 5.009 g (14.80 mmol) $Eu(NO_3)_3\cdot 6H_2O$ in 50 mL ethanol and adding a solution of 2.027 g phen in 20 mL ethanol. The colorless precipitate was obtained after 1 d (32% yield). The $[Cr(phen)_2Cl_2]Cl$ complex was synthesized by refluxing a mixture of 0.040 g (2.5 mmol) $CrCl_3\cdot 6H_2O$, 0.010 g (1.5 mmol) Zn powder in 25 mL methanol for 20 min. Subsequently 0.901 g (5.0 mmol) phen were added and refluxed for 1 h.[51]

Synthesis of **II**: 0.167 g (0.055 mmol) of **I** were mixed with 0.1140 g (0.165 mmol) of $[Ni(phen)_3](ClO_4)_2\cdot 0.5H_2O$ in 4 mL dist. $H_2O$ and heated at 150 °C for 1 d. Yield: 83%, based on V. Elemental analyses: C 23.14, H 2.34, N 5.62%; calcd for $C_{76}H_{104}Ni_3N_{16}O_{62}Sb_6V_{15}$: C 23.38, H 2.34, N 5.74%.

Further experiments were performed to investigate the ligand exchange reaction (reaction time: 1 d; $T$ = 150 °C). Varying the amount of $[Ni(phen)_3](ClO_4)_2\cdot 0.5H_2O$ from 50 to 150% always afforded crystallization of **II** with no significant changes of the yield. However, using larger concentrations of the complex leads to crystallization of the excess together with compound **II**. Adding en (0.1–0.5 mL) blocks the formation of **II**.

When using $[Eu(phen)_2(NO_3)_3]$ or $[Cr(phen)_2Cl_2]Cl$ as precursor complexes, compound **II** is formed. Most importantly, adding only phen instead of any preformed complexes also leads to crystallization of **II**. Applying a large excess of phen (0.33–0.66 mmol) formation of **II** is also observed.

Compound **II** was characterized by elemental (CHN) analysis, energy dispersive X-ray analysis (EDX), differential thermoanalysis and thermogravimetry (DTA-TG) and IR spectroscopy as well as single crystal structure analysis (see ESI Fig. S1–S3 and Tables S1, S2†). X-ray powder diffraction patterns (XRPD) of the products obtained after the different syntheses are displayed in Fig. S4 and S5.† All chemicals were purchased ($NH_4VO_3$, $NiCl_2\cdot 6H_2O$, $Sb_2O_3$, $CrCl_3\cdot 6H_2O$, $Eu(NO_3)_3\cdot 6H_2O$ (Merck), ethylenediamine (Fluka), phenanthroline, $Ni(ClO_4)_2\cdot 6H_2O$ (ABCR)) and used without further purification.

### Spectroscopic investigations

The IR spectra were measured in the 400–4000 cm$^{-1}$ range using a Genesis FTIRTM spectrometer (ATI Mattson).

### Elemental analysis

CHN analyses were performed using an EURO EA Elemental Analyzer from EURO VECTOR Instruments.

### Differential thermoanalysis and thermogravimetry

Thermogravimetry analysis were performed in $Al_2O_3$ crucibles using a Netzsch STA-409CD instrument heating the sample under a nitrogen atmosphere with a constant flow rate of 75 mL min$^{-1}$ and a heating rate of 1 K min$^{-1}$.

### EDX analyses

EDX measurements were performed using a Philips Environmental Scanning Electron Microscope ESEM XL30 equipped with an EDAX detector.

### X-ray powder diffraction

The X-ray powder patterns were recorded using a STOE STADI-P diffractometer (transmission geometry, Cu-Kα radi-

ation ($\lambda$ = 1.540598 Å)) to determine the phase purity of the reaction product comparing the experimental pattern with that calculated from single crystal X-ray data.

### Magnetic measurements

A Quantum Design MPMS-5XL SQUID magnetometer was used to collect magnetic susceptibility data of **II**. The polycrystalline sample was compacted and immobilized into cylindrical PTFE capsules. The data were acquired as a function of the field (0.1–5.0 T at 2.0 K) and temperature (2.0–290 K at 0.1 T). The data were corrected for the diamagnetic contributions of the sample holder and the compound ($\chi_{dia}$ = −1.93 × $10^{-3}$ $cm^3$ $mol^{-1}$).

### Single crystal structure analysis

Data collection was performed with a STOE Imaging Plate Diffraction System (IPDS-1) with Mo-$K_\alpha$ radiation ($\lambda$ = 0.71073 Å). A numerical absorption correction was performed ($T_{min/max}$: 0.5232/0.7241). The crystal structure was solved with the SHELXS-97 [51] and refined against $F^2$ using SHELXL-2014.[52] All non H atoms were refined anisotropic. The C–H and N–H H atoms were positioned with idealized geometry and refined isotropic using a riding model. Most of the O–H H atoms were located in difference maps, their bond lengths were set to ideal values and finally, they were refined isotropic using a riding model. One water molecule is disordered over two positions and was refined using a split model. Two additional water positions are not fully occupied. For the last three O atoms the H atoms could not be located but were considered in the calculation of the formula.

Crystallographic data (excluding structure factors) for the structure in this paper have been deposited with the CCDC (No. 1504150).

## Acknowledgements

We thank the state of Schleswig-Holstein for financial support. The work has been in part funded by ERC grant 308051 – MOLSPINTRON.

## References

1 K. Y. Monakhov, W. Bensch and P. Kögerler, *Chem. Soc. Rev.*, 2015, **44**, 8443.
2 G. Zhou, Y. Xu, C. Guo, Y. Liu and X. Zheng, *J. Cluster Sci.*, 2007, **18**, 388.
3 A. Müller and J. Döring, *Z. Anorg. Allg. Chem.*, 1991, **595**, 251.
4 A. Wutkowski, N. Evers and W. Bensch, *Z. Anorg. Allg. Chem.*, 2011, **637**, 2205.
5 A. Müller, J. Döring, M. I. Khan and V. Wittneben, *Angew. Chem., Int. Ed. Engl.*, 1991, **30**, 210.
6 A. Müller and J. Döring, *Angew. Chem., Int. Ed. Engl.*, 1988, **27**, 1721.
7 M. I. Khan, Q. Chen and J. Zubieta, *Inorg. Chim. Acta*, 1993, **212**, 199.
8 B. Chen, B. Wang, W. Lin, L. Fan, Y. Gao, Y. Chi and C. Hu, *Dalton Trans.*, 2012, **41**, 6910.
9 G. Zhou, C. Guo, W. Liu, Y. Xu and X. Zheng, *J. Coord. Chem.*, 2008, **61**, 202.
10 X.-B. Cui, J.-Q. Xu, Y. Li, Y.-H. Sun, L. Ye and G.-Y. Yang, *J. Mol. Struct.*, 2003, **657**, 397.
11 S.-Y. Shi, Y. Chen, J.-N. Xu, Y.-C. Zou, X.-B. Cui, Y. Wang, T.-G. Wang, J.-Q. Xu and Z.-M. Gao, *CrystEngComm*, 2010, **12**, 1949.
12 S.-T. Zheng, J. Zhang and G.-Y. Yang, *Z. Anorg. Allg. Chem.*, 2005, **631**, 170.
13 S.-T. Zheng, J.-Q. Xu and G.-Y. Yang, *J. Cluster Sci.*, 2005, **16**, 23.
14 S.-T. Zheng, Y.-M. Chen, J. Zhang, J.-Q. Xu and G.-Y. Yang, *Eur. J. Inorg. Chem.*, 2006, 397.
15 S.-T. Zheng, J. Zhang, B. Li and G.-Y. Yang, *Dalton Trans.*, 2008, 5584.
16 L. Zhang, X. Zhao, J. Xu and T. Wang, *J. Chem. Soc., Dalton Trans.*, 2002, 3275.
17 E. Antonova, C. Näther, P. Kögerler and W. Bensch, *Angew. Chem., Int. Ed.*, 2011, **50**, 764.
18 A. Wutkowski, C. Näther, P. Kögerler and W. Bensch, *Inorg. Chem.*, 2008, **47**, 1916.
19 M. Wendt, U. Warzok, C. Näther, J. van Leusen, P. Kögerler, C. A. Schalley and W. Bensch, *Chem. Sci.*, 2016, **7**, 2684.
20 L. Yu, J.-P. Liu, J.-P. Wang and J.-Y. Niu, *Chem. Res. Chin. Univ.*, 2009, **25**, 426.
21 M. Wendt, C. Näther and W. Bensch, *Chem. – Eur. J.*, 2016, **22**, 7747.
22 E. Antonova, C. Näther, P. Kögerler and W. Bensch, *Angew. Chem., Int. Ed.*, 2011, **123**, 790.
23 R. Kiebach, C. Näther, P. Kögerler and W. Bensch, *Dalton Trans.*, 2007, 3221.
24 E. Antonova, C. Näther and W. Bensch, *Dalton Trans.*, 2012, **41**, 1338.
25 E. Antonova, C. Näther and W. Bensch, *CrystEngComm*, 2012, **14**, 6853.
26 E. Antonova, C. Näther, P. Kögerler and W. Bensch, *Inorg. Chem.*, 2012, **51**, 2311.
27 A. Wutkowski, C. Näther, P. Kögerler and W. Bensch, *Inorg. Chem.*, 2013, **52**, 3280.
28 M. O'Keeffe and N. E. Brese, *J. Am. Chem. Soc.*, 1991, **113**, 3226.
29 X.-X. Hu, J.-Q. Xu, X.-B. Cui, J.-F. Song and T.-G. Wang, *Inorg. Chem. Commun.*, 2004, **7**, 264.
30 A. Wutkowski, C. Näther and W. Bensch, *Inorg. Chim. Acta*, 2011, **379**, 16.
31 M. S. Deshpande, A. S. Kumbhar and C. Näther, *Dalton Trans.*, 2010, **39**, 9146.
32 G. Laus, V. Kahlenberg, K. Wurst, T. Lörting and H. Schottenberger, *CrystEngComm*, 2008, **10**, 1638.
33 E. Freire, S. Baggio, J. C. Munoz and R. Baggio, *Acta Crystallogr., Sect. C: Cryst. Struct. Commun.*, 2002, **C58**, m221.
34 Z.-H. Xu, X.-F. Li and X.-W. Zhang, *Synth. React. Inorg., Met.-Org., Nano-Met. Chem.*, 2012, **42**, 140.

 

35 L. Infantes and S. Motherwell, *CrystEngComm*, 2002, **4**, 454.
36 L. Infantes, J. Chisholm and S. Motherwell, *CrystEngComm*, 2003, **5**, 480.
37 L. Infantes, L. Fabian and W. D. S. Motherwell, *CrystEngComm*, 2007, **9**, 65.
38 J. Hilbert, C. Näther and W. Bensch, *Inorg. Chem.*, 2015, **53**, 5619.
39 S. Grimme, *Angew. Chem., Int. Ed.*, 2008, **47**, 3430.
40 J. W. G. Bloom and S. W. Wheeler, *Angew. Chem.*, 2011, **123**, 7993, (*Angew. Chem., Int. Ed.*, 2011, **50**, 7847).
41 Y.-H. Chi, J.-M. Shi, H.-N. Li, W. Wei, E. Cottrill, N. Pan, H. Chen, Y. Liang, L. Yu, Y.-Q. Zhang and C. Hou, *Dalton Trans.*, 2013, **42**, 15559.
42 C. A. Hunter, K. R. Lawson, J. Perkins and C. J. Urch, *J. Chem. Soc., Perkin Trans. 2*, 2001, 651.
43 R. Kiebach, C. Näther and W. Bensch, *Solid State Sci.*, 2006, **8**, 964.
44 E. Antonova, A. Wutkowski, C. Näther and W. Bensch, *Solid State Sci.*, 2011, **13**, 2154.
45 E. Antonova, C. Näther, P. Kögerler and W. Bensch, *Dalton Trans.*, 2012, **41**, 6957.
46 Y. Gao, Z. Han, Y. Xu and C. Hu, *J. Cluster Sci.*, 2010, **21**, 163.
47 H. Lueken, *Magnetochemie*, Teubner, Stuttgart, 1999.
48 M. Speldrich, H. Schilder, H. Lueken and P. Kögerler, *Isr. J. Chem.*, 2011, **51**, 215.
49 J. van Leusen, M. Speldrich, H. Schilder and P. Kögerler, *Coord. Chem. Rev.*, 2015, **289**, 137.
50 L. Abdel-Rahman, L. P. Battaglia, C. Rizzoli and P. Sgarabotto, *J. Chem. Crystallogr.*, 1995, **25**, 629.
51 X. Gao, *Acta Crystallogr., Sect. E: Struct. Rep. Online*, 2011, **67**, m139.
52 G. M. Sheldrick, *Acta Crystallogr., Sect. A: Fundam. Crystallogr.*, 2008, **64**, 112.